Eur. Phys. J. B **14**, 217–226 (2000)

THE EUROPEAN PHYSICAL JOURNAL B

EDP Sciences

Born effective charge reversal and metallic threshold state at a band insulator-Mott insulator transition

N. Gidopoulos[1,2], S. Sorella[1,2,a], and E. Tosatti[1,2,3,b]

[1] International School for Advanced Studies (SISSA), Via Beirut 2-4, 34014 Trieste, Italy
[2] Istituto Nazionale di Fisica della Materia (INFM), Unita' Trieste SISSA, 34014 Trieste, Italy
[3] International Centre for Theoretical Physics, P.O. Box 586, 34014 Trieste, Italy

Received 21 May 1999

Abstract. We study the quantum phase transition between a band ("ionic") insulator and a Mott-Hubbard insulator, realized at a critical value $U = U_c$ in a bipartite Hubbard model with two inequivalent sites, whose on-site energies differ by an offset Δ. The study is carried out both in $D = 1$ and $D = 2$ (square and honeycomb lattices), using exact Lanczos diagonalization, finite-size scaling, and Berry's phase calculations of the polarization. The Born effective charge jump from positive infinity to negative infinity previously discovered in $D = 1$ by Resta and Sorella is confirmed to be directly connected with the transition from the band insulator to the Mott insulating state, in agreement with recent work of Ortiz *et al.* In addition, symmetry is analysed, and the transition is found to be associated with a reversal of inversion symmetry in the ground state, of magnetic origin. We also study the $D = 1$ excitation spectrum by Lanczos diagonalization and finite-size scaling. Not only the spin gap closes at the transition, consistent with the magnetic nature of the Mott state, but also the charge gap closes, so that the intermediate state between the two insulators appears to be metallic. This finding, rationalized within Hartree-Fock as due to a sign change of the effective on-site energy offset Δ for the minority spin electrons, underlines the profound difference between the two insulators. The band-to-Mott insulator transition is also studied and found in the same model in $D = 2$. There too we find an associated, although weaker, polarization anomaly, with some differences between square and honeycomb lattices. The honeycomb lattice, which does not possess an inversion symmetry, is used to demonstrate the possibility of an inverted piezoelectric effect in this kind of ionic Mott insulator.

PACS. 75.10.Jm Quantized spin models – 71.20.-b Electron density of states and band structure of crystalline solids – 71.27.+a Strongly correlated electron systems; heavy fermions

1 Introduction

Standard discussions of the Mott-Hubbard transition are generally concerned with lattices of equivalent sites. At zero temperature, the metal-insulator transition develops when the on-site electron-electron repulsion U reaches some critical value U_c which, usually, also corresponds to the onset of characteristic magnetic correlations. In this paper we are concerned with the less common case where the system is ionic, encompassing "anions" and "cations". Earlier workers, including Nagaosa and Takimoto [1], and Egami, Ishihara and Tachiki [2] considered the simplest two-site ionic generalization of the Hubbard model (henceforth dubbed Ionic Hubbard Model, IHM), which exhibits the transition from a band insulator to a Mott insulator. Such a system is, in the absence of electron-electron repulsions, $U = 0$, a regular band insulator. As U increases above some critical value U_c, a band insulator Mott-Hubbard insulator transition is expected to take place. When U is sufficiently large, the inequivalence between anion and cation should in fact become irrelevant, and the ground state of a large U system of equivalent sites is Mott-insulating, with antiferromagnetic correlations. However, owing to the residual inequivalence of the two ionic sites, it will also exhibit other properties, which have only partly been explored so far. Of special interest is the anomalous behaviour of the polarization of the ionic solid across the transition. A very interesting quantity in this regard is the Born effective charge Z^* associated with an infinitesimal "dimerizing" displacement of the ionic lattice, corresponding to a frozen $q = 0$ optical phonon. Resta and Sorella [3] studied the IHM in $D = 1$ using Lanczos diagonalization and found, by the Berry phase method, very striking indications of a polarization anomaly at $U = U_c$. Ortiz, Ordejón, Martin and Chiappe [4] proposed a simple Hartree-Fock explanation to the anomaly, namely that at a first order magnetic

[a] e-mail: sorella@sissa.it
[b] e-mail: tosatti@sissa.it

transition between an AF insulator and a band magnetic insulator, the polarization may also abruptly jump.

A number of important questions are apparently still open at this stage, in particular

1. What is the physical origin of the polarization anomaly at the band-Mott transition, and what is its connection with symmetry?
2. What is the nature precisely at $U = U_c$, of the "threshold" state between the band and the Mott insulator?
3. How does the polarization anomaly depend on the dimensionality? In particular, will it survive in 2D and 3D, and if so, with what strength?
4. Bearing in mind that most experiments measure just only Z^{*2}, can we identify a simple experimentally accessible quantity which could signal the Z^* anomaly in magnitude and sign?

In this paper we set out to discuss principally these questions. We will do it by studying more closely the same simple ionic Hubbard model [2–4], in particular by analysing the symmetry of its possible ground states, by calculating effective charges and excitation spectra, and generally by seeking to understand its properties by exact diagonalizations supplemented when necessary by the simple Hartree-Fock approximation.

Firstly, we find that the Mott insulator does, for appropriate boundary conditions, possess odd symmetry under inversion, contrary to the ionic band insulator, which has even parity. Secondly, Hartree-Fock reveals that one clue to the polarization anomaly lies in an effective reversal of the on-site energy offset (accompanied with the vanishing of the associated band gap), taking place for the minority spin species only at U_c. Thirdly, in agreement with Hartree-Fock, exact results suggest that at U_c not only the spin gap but also the true charge gap vanishes, indicating a metallic "threshold" state poised precisely at the brink between the band insulator and the Mott insulator. Fourthly, a fresh study of two different 2D lattices, namely square and honeycomb, shows that a direct band insulator-Mott-Hubbard insulator transition and the associated polarization anomaly may survive in higher dimensions too, particularly in the 2D honeycomb lattice. Here, the anomaly is weaker than in $D = 1$ (a jump instead of a divergence). Finally, we propose the piezoelectric effect in a non-centrosymmetric lattice, here exemplified precisely by the 2D honeycomb lattice, as the experimentally accessible quantity that will directly and strikingly change sign at the band insulator-Mott insulator transition.

The polarization calculations are carried out using the Berry phase technique, first introduced by King-Smith and Vanderbilt [5] and by Resta [6], and further extended to a general many-body case by Ortiz and Martin [7], and applied to the IHM by Resta and Sorella.

The rest of this paper is structured as follows. In Section 2 we introduce the ionic Hubbard model and describe briefly the classical limit, $t = 0$, useful for understanding later the full quantum case. In Section 3 we first present a discussion of the magnetic behavior expected by the model, followed by a more detailed discussion of symmetry, and by a finite-size study of the level crossings connected with the transition at U_c. Section 4 contains the Hartree-Fock theory of the band-Mott insulator transition, and of the polarization anomaly. Section 5 presents the full many-body calculation of the polarization, done by means of Lanczos diagonalization plus Berry phase, here specialized to the 2D honeycomb case, and finally in Section 6 we give a discussion of the possible detectability of the transition *via* the piezoelectric effect, followed by our general conclusions.

2 Ionic Hubbard model

We consider the Hubbard Hamiltonian in 1D (linear chain) and 2D bipartite lattices (square and honeycomb lattices). All lattices being bipartite, they are composed of A and B sublattices. To simulate ionicity, A and B are made inequivalent by onsite energies $\frac{\Delta}{2}$ and $-\frac{\Delta}{2}$ respectively. Because of the energy difference Δ between the A and the B sublattices, the electron population of the A sublattice is less than that of the B sublattice for $\Delta > 0$ (or *vice versa* for $\Delta < 0$). The sublattices are connected by electron hopping. We assume a filling of one electron per site. Sites of the A sublattice are denoted by R_A, those of the B sublattice by $R_B = R_A + \xi_\mu$, where the vectors ξ_μ connect an A site with its neighbouring B sites, $\mu = 1, 2, \ldots, \nu$. In the linear chain, where the length of the unit cell is 2, μ = 0,1, $\xi_{0,1} = \pm 1$. In the square lattice (square side of unit length), μ = 0,1,2,3 and $\xi_{0,2} = \pm(1,0)$, $\xi_{1,3} = \pm(0,1)$. In the honeycomb lattice (unit length is the side of the hexagon), μ = 0,1,2 and $\xi_0 = (-\frac{1}{2}, \frac{\sqrt{3}}{2})$, $\xi_1 = (1, 0)$, $\xi_2 = (-\frac{1}{2}, -\frac{\sqrt{3}}{2})$. The Hamiltonian is

$$H = -\sum_{R_A,\mu,\sigma} t_\mu c^\dagger_{R_A+\xi_\mu,\sigma} c_{R_A,\sigma} + \text{h.c.} + U \sum_R n_{R\uparrow} n_{R\downarrow} + \frac{\Delta}{2}\left[\sum_{R_A,\sigma} c^\dagger_{R_A,\sigma} c_{R_A,\sigma} - \sum_{R_B,\sigma} c^\dagger_{R_B,\sigma} c_{R_B,\sigma}\right] \quad (1)$$

where we have used standard notation, and U is the Hubbard onsite electron-electron repulsive interaction. Electrons hop with matrix elements $-t_\mu (t_\mu > 0)$ between neighbouring sites from the A to the B sublattice along the ξ_μ directions. We denote the ground state energy of our N-electron system as $E(N)$. When in need to distinguish between the number of spin up and spin down electrons, the ground state energy will be denoted by $E(N\uparrow, N\downarrow)$. Unless otherwise specified $N\uparrow = N\downarrow = N/2$. We shall study the charge gap and the spin gap of the system defined respectively as: $\Delta E_{\text{charge}} = E(N+1) + E(N-1) - 2E(N)$ and $\Delta E_{\text{spin}} = E(N\uparrow + 1, N\downarrow - 1) - E(N\uparrow, N\downarrow)$.

2.1 Behavior in the classical limit, t = 0

It is instructive at the outset to consider what happens when all $t_\mu = 0$. As sketched in Figure 1 if we set the hopping $t_\mu = 0$ in the Hamiltonian (1) the model is classical.

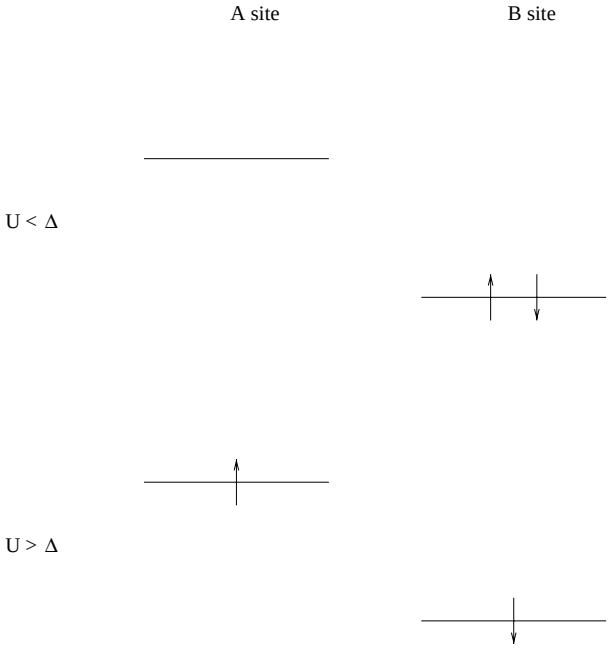

Fig. 1. The model at the classical level when the hopping t is set to zero. The energy difference between an A site and a B site is Δ. At one electron per site filling, when the onsite interaction $U < \Delta$ the B site is doubly occupied and the A site empty. When $U > \Delta$ both sites are single occupied.

It has a first order transition at $U = \Delta$ with a change of the macroscopic polarization per unit cell $\Delta P = ea/2$. Both the charge and spin gaps are finite and coincide in the region $U < \Delta$ where they are given by $\Delta E = \Delta - U$. For $U > \Delta$ the charge gap remains finite $\Delta E_{\text{charge}} = U - \Delta$ while the spin gap vanishes. Note that precisely at $U = \Delta$, where the transition takes place, both the charge and the spin gap vanish. This kind of transition expected to persist for $t > 0$, where it takes a standard band insulator, with a charge and a spin gap, over to an antiferromagnetic insulator, with a charge gap, and gapless spin excitations for large U.

3 Magnetism, symmetry, level crossing and polarization jump

In this section we discuss the polarization properties of an electron system close to an antiferromagnetic transition. As discussed by Ortiz and Martin antiferromagnetism appears to play a crucial role and remarkably affects the behaviour of the polarization [4].

Let us consider a finite electron hopping t_μ. For $U = 0$, one electron per site, the model is in fact described by a completely filled, spin independent band, separated by a finite gap ($\sim \Delta$, for large Δ) from the second, empty band. In the opposite limit of large U the standard strong coupling analysis of the Hubbard model leads to a charge gap $\sim U$, and to the well-known Heisenberg Hamiltonian [8] H_J for spins:

$$H_J = J \sum_{\langle i,j \rangle} \mathbf{S}_i \cdot \mathbf{S}_j \tag{2}$$

with an antiferromagnetic superexchange coupling $J = \frac{4t^2}{U}$. The mapping to the Heisenberg model implies that for large U the model has gapless spin excitations. In one dimension they have been named "spinons" [8], and can be derived from the exact Bethe ansatz solution of the 1D Heisenberg model [9]. In higher dimensions, where antiferromagnetic long range order is believed to exist at $T = 0$ in 2D [10–12] and 3D [13], the gapless modes are spin waves.

A band insulator-Mott insulator transition should therefore occur at some finite coupling U_c. Of course, U_c will differ from its classical value $U_c^0 = \Delta$. There will be in general the possibility of intermediate metallic phases covering a range of U values. Even if the insulator-insulator transition is direct, quantum fluctuations may drive its character, for example from first order to second order, or else may split it into more than one transition [14]. Quantum antiferromagnets with long range order for $U > U_c$ (or quasi long range order in one dimension) can be described at the critical level, by the well-known non linear sigma model, with action

$$S = \frac{1}{2g} \int \mathrm{d}x^{d+1} (\boldsymbol{\nabla} \mathbf{n})^2 \tag{3}$$

where $\mathbf{n}$ is a unit vector describing the local orientation of the antiferromagnetic order parameter, and the coupling constant g depends on the microscopic parameters U, Δ of the model. This effective model is well-known to have a second order transition predicting that a spin gap opens up continuously for $g > g_c$, alias $U < U_c$ [12].

We will for simplicity assume in the following that the transition is unique and is always second order even though a Hartree-Fock calculation [4] in the one-dimensional model and our own in the 2D square lattice indicates the opposite. In fact, the Hartree-Fock approximation may fail anyway to describe correctly the order of the transition, as it is not appropriate to describe the gapless spin-wave excitations of the model in the ordered phase. Contrary to the linear chain and the square lattice, the Hartree-Fock method however correctly predicts (see Sect. 4) a second order phase transition in the honeycomb lattice, at least for the parameter values studied here.

The magnetic Mott insulator for $U > U_c$ has a charge gap, and is therefore fully described by the nonlinear sigma model, at least in more than one dimensions. This model does not present any further phase transition but the one at the critical coupling g_c, which is thus related to U_c. It is possible however that the charge transition to a band insulator might occur for U values different from U_c, as suggested by Fabrizio *et al.* [14]. We shall return to this point below.

3.1 D = 1: symmetry, level crossing and critical U_c

In a finite system with -say- L sites a level crossing may occur for some particular boundary conditions, if allowed by symmetry. In particular, in the one-dimensional model, it can be easily proved that there exists a finite value $U_c(L)$ at which the ground state undergoes a change in the eigenvalue of the inversion symmetry operator R. Inversion symmetry around the site $i = 0$ is defined by the following relations:

$$Rc^\dagger_{i,\sigma}R^\dagger = c^\dagger_{L-i,\sigma} \quad \text{for} \quad i = 0, 1, \cdots L-1 \tag{4}$$

$$R|0\rangle = |0\rangle \tag{5}$$

where $|0\rangle$ is the electron vacuum state, by definition invariant under inversion symmetry.

The additional relation (5) is necessary to completely define the inversion transformation $\hat{R}$ in the whole Hilbert space. Inversion does not interchange the A and the B sublattice and clearly commutes with the Hamiltonian (1) for any U, provided the boundary conditions are real, namely periodic or antiperiodic (see Sect. 5).

Since $R^2 = I$, the identity, the inversion has obviously two eigenvalues, ± 1. We will show in the following that the ground state $|\psi_0\rangle_U$ satisfies $R|\psi_0\rangle_U = |\psi_0\rangle_U$ for $U = 0$, whereas for large U there is a change of sign and $R|\psi_0\rangle_U = -|\psi_0\rangle_U$, so that a level crossing must occur at an intermediate coupling $U = U_c(L)$.

In the non-interacting system the ground state is a direct product of a spin up and a spin down Slater determinants, both possessing the same orbitals of the lowest band. Both Slater determinants have a definite parity $R_\sigma = \pm 1$ and the inversion eigenvalue of the global wavefunction is given by their product

$$R = R_\uparrow \times R_\downarrow = 1.$$

Hence the band insulating state is even under inversion.

In the large-U Mott insulator instead we can use the mapping to the Heisenberg Hamiltonian (2), whose ground state in arbitrary dimensions can be generally written as [13]:

$$|\psi_0\rangle_{U\to\infty} = \sum_{i_1, i_2, \cdots i_{L/2}} \Phi(i_1, i_2, \cdots i_{L/2}) S^-_{i_1} S^-_{i_2} \cdots S^-_{i_{L/2}} |F\rangle$$

where $S^-_i = c^\dagger_{\downarrow i} c_{\uparrow i}$ is the spin lowering operator at the site i, $|F\rangle = \prod_i c^\dagger_{\uparrow,i}|0\rangle$ is the ferromagnetic state along the spin-up direction, and the wavefunction Φ is real. Φ is also subject to the well known ("Marshall sign") condition [13], *i.e.* the sign of the wavefunction is determined by the number of spin flips in the B sublattice (i odd):

$$\Phi(i_1, i_2, \cdots, i_{L/2})(-1)^{\Sigma_{k=1}^{L/2} i_k} > 0.$$

The action of the inversion symmetry R on the spin lowering operators can be easily found by applying the definition given in equations (4, 5), namely $RS^-_i R^\dagger = S^-_{L-i}$, and thus R maps an element of the basis $S^-_{i_1} S^-_{i_2} \cdots S^-_{i_{L/2}}|F\rangle$ to another one $S^-_{i'_1} S^-_{i'_2} \cdots S^-_{i_{L/2}} R|F\rangle$ where $i' = L - i$ and $R|F\rangle = \prod_i c^\dagger_{L-i}|0\rangle = \pm|F\rangle$. The overall sign $\pm$ in the latter equation represents just the inversion eigenvalue of the ferromagnetic state $|F\rangle$ and can be determined using the canonical anticommutation rules to restore the order of the creation operators $c^\dagger_i$ after the application of the inversion operator R to the ferromagnetic state $|F\rangle$. Since inversion symmetry does not change the Marshall sign we arrive to the conclusion that the inversion eigenvalue of the Heisenberg wavefunction coincides with the inversion eigenvalue of the ferromagnetic state $|F\rangle$ which is simple to compute.

In this way we find that for $U \to \infty$, the inversion eigenvalue can change sign depending on the boundary conditions (b.c.):

$$\begin{aligned} R &= (-1)^{L/2+1} && \text{for periodic b.c.} \\ R &= (-1)^{L/2} && \text{for antiperiodic b.c.} \end{aligned} \tag{6}$$

This finally proves our initial statement; in particular a level crossing from an even state to an odd one has to occur in a periodic ring with $L = 4n$ or in an antiperiodic one with $L = 4n + 2$. On the other hand, there will not necessarily be a level crossing in a periodic ring with $L = 4n + 2$ and an antiperiodic one with $L = 4n$. In summary, we conclude that the demise of the band insulator occurs *via* a symmetry change, whose finite-size signature is a parity switch from even to odd in the appropriate boundary conditions.

3.2 Consequences on the calculation of the polarization

As will be discussed in Section 5 the change of polarization in a many-body system can be obtained using a form of averaging over the boundary conditions. Thus the averaging necessarily include both periodic (PBC) and antiperiodic (APBC) boundary conditions. Now, in one or in the other, depending on L, a level crossing will necessarily occur at some finite $U_c(L)$. From the theory of polarization a strong variation of the polarization can be expected as a function of U around $U_c(L)$ even in presence of a perturbations such as a dimerization δ (see Sect. 5). Therefore, within the hypothesis that there exists only a well defined Mott transition at a critical value U_c in the thermodynamic limit, we may expect that:

$$U_c(L) \to U_c \quad \text{for } L \to \infty \tag{7}$$

that is, the U value where the level crossing occurs for large size is just the critical value of the magnetic transition.

3.3 Charge and spin gaps in D = 1

Understanding charge and spin excitation gaps is a crucial point. We have studied these quantities in the $D = 1$ case

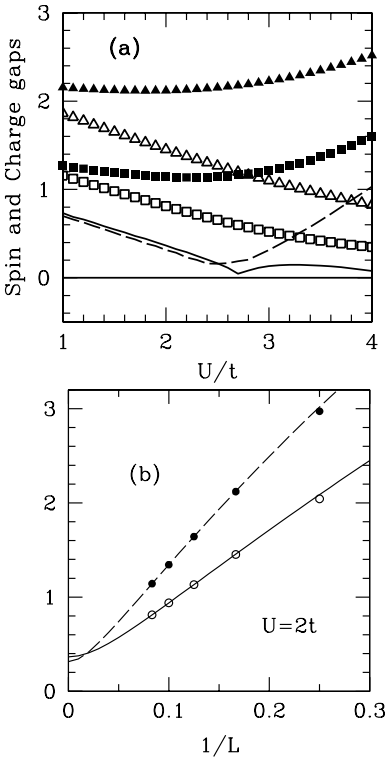

Fig. 2. (a) Calculation on 12 site rings (squares) and 6 site rings (triangles) of the charge (black) and spin (white) gaps, using closed shells at fillings of one electron per site. The data of the gaps for the 8, 10 (not shown) and 12 sites are used for a finite size scaling extrapolation to the infinite number of sites. The curves of the charge (dashed line) and spin (solid line) gaps are shown. The two gaps seem to coincide in the region below U_c. Near U_c where the spin gap is closing, the charge gap is also (nearly) closing. (b) Finite size scaling for $U/t = 2$. Black dots and open circles denote charge and spin gaps respectively.

as a function of U/t, performing calculations on finite rings with PBC or APBC. By considering the sequence of closed shells with one electron per site, there is no level crossing and a finite size scaling analysis can be safely applied to the charge and spin gaps (see the end of Sect. 2 for their definitions). For a general finite size system, the lowest order correction to any gap should be of the form $\frac{A}{L^2}$. We have used a three parameter fit

$$\Delta_L = \sqrt{\Delta^2 + \frac{A}{L^2} + \frac{B}{L^3} + \dots} \tag{8}$$

including also a higher order L^{-3} term, to improve the accuracy. In Figure 2 we show the finite size calculations of the gaps for the 6 and the 12 site ring, as well as the result extrapolated to the thermodynamic limit with the finite size scaling (8). In Figure 3 we also present the results for the spin and charge gaps for open shell rings of 6 and 12 sites. The overall behavior of the gaps for the largest open shell ring ($L = 12$) is in agreement with the infinite size extrapolation of the closed shell rings, supporting the validity of our finite size scaling. Starting with the band

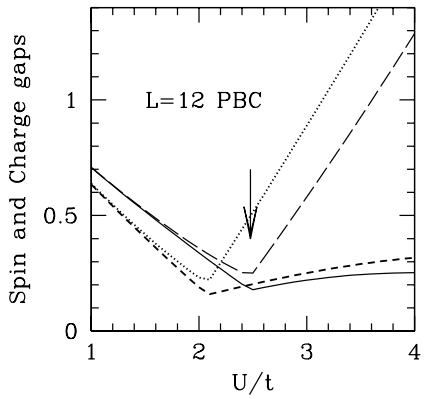

Fig. 3. Calculation on 12 site rings (solid and long dashed line) and 6 site rings (short dashed and dotted lines) of the charge (long dashed and dotted lines) and spin (solid and short dashed lines) gaps, using open shells at fillings of 1 electron per site. The results of the 12 site calculation practically coincide with the finite size scaling results of the closed shells.

insulator at small U, and increasing U, we find that both charge and spin gaps are very close, and decrease together until they appear to close at some U_c. For $U > U_c$, the charge gap turns sharply upwards, while the spin gap does not. Precisely at $U_c \simeq 2.75t$, our fit suggests finite size gap corrections of the form $\frac{1}{L}$, which implies not only spin, but also charge gapless excitations. This being the case, the system at U_c is metallic. The nature of this metal is unknown and deserves further investigation [15].

From our calculations it is hard to say whether charge and spin gaps will vanish at exactly the same U_c, or at two slightly different values, as very recently proposed in [14]. Nonetheless it is suggestive that large finite size charge gaps and small spin gaps become slightly inverted after extrapolation (see Fig. 2b), which goes precisely in the direction of a charge gap closing at a slightly smaller U than the spin gap.

We defer all discussion of the possible two-transition scenario to the work of Fabrizio *et al.* [14] and we will not further dwell on it in this paper, where we consider for simplicity a single U_c.

3.4 Extension to higher dimensions: D = 2

In the previous analysis of a level crossing in the model (1) we did not explicitly use the exact Bethe ansatz solution of 1D systems. In fact the result that the inversion symmetry R for large U has the same eigenvalue of the corresponding ferromagnetic state $|F\rangle$ remains valid also in $D = 2$, and so does the evenness of the band insulator at small U.

Unfortunately, unlike $D = 1$, the $D = 2$ inversion symmetry, transforming $(x, y) \to (L-1-x, L-1-y)$ leaves the ferromagnetic state invariant on a bipartite lattice. Thus, a level crossing cannot be argued based on identically the same symmetry argument. As it turns out, however, it is again possible to generalize the argument by using a more elaborate symmetry operator, which changes eigenvalue in going from the $U = 0$ state to large U state. In the square

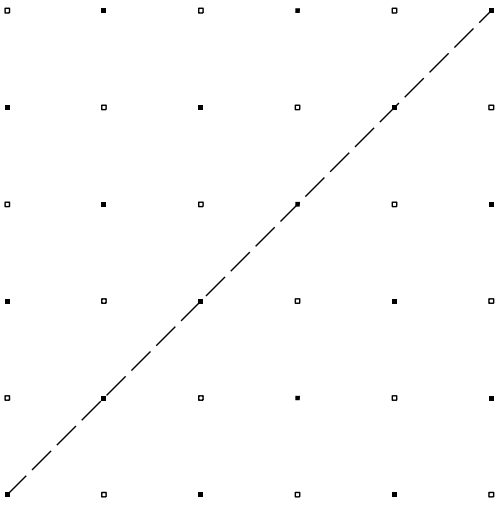

Fig. 4. Square lattice of side l with $l/2$ odd. The number of lattice sites which lie on either side of the diagonal is odd.

lattice this symmetry operator is easily identified. It is the mirror symmetry across the diagonal of the square lattice $L = l \times l$ with $l/2$ odd (see Fig. 4). In the honeycomb lattice one can also find a symmetry operation with the same property. However, it is much more involved and we will not discuss it in detail here. We only mention that this symmetry is obtained by a 120° rotation around a site followed by an additional gauge transformation $c_i^\dagger \to c_i^\dagger e^{j\theta_i}$ with suitable angles θ_i [16].

Based on this analysis, we can therefore conclude that, upon averaging over the boundary conditions, there will be, both in the square and in the honeycomb lattice, a level crossing when the system is in the Mott state, but none in the band insulator state. Therefore, we should expect a polarization anomaly, and a metallic state at the transition, also in these two-dimensional cases.

However, before moving on to do numerical work and check these expectations in these more difficult problems, it is wise to solve them in simple mean-field which, as the $D = 1$ case demonstrated [4], is always very instructive.

4 2D bipartite lattices: Hartree-Fock approximation

We shall consider the Hubbard model on the bipartite honeycomb lattice, defined in Section 2, and on the simpler square lattice. In the latter case, in order to remove the nesting degeneracy of the non interacting 2D Fermi surface, we have also studied the effect of the next-nearest neighbour hopping.

In the Hartree-Fock approximation the ground state of the Hamiltonian is approximated by a Slater determinant. We may further assume that this Slater determinant $|SD\rangle$ is factored in spin space

$$|SD\rangle = |SD_\uparrow\rangle \otimes |SD_\downarrow\rangle. \tag{9}$$

With this choice it is simple to obtain the Hartree-Fock Hamiltonian by linearizing the interaction term:

$$\begin{aligned} Un_\uparrow n_\downarrow = U\left(\langle SD_\downarrow|n_\downarrow|SD_\downarrow\rangle n_\uparrow + \langle SD_\uparrow|n_\uparrow|SD_\uparrow\rangle n_\downarrow\right) \\ - U\langle SD_\downarrow|n_\downarrow|SD_\downarrow\rangle\langle SD_\uparrow|n_\uparrow|SD_\uparrow\rangle. \end{aligned}$$

In this way we obtain:

$$H_{\mathrm{Hartree-Fock}} = H_\uparrow + H_\downarrow + E_{\mathrm{const}}$$

where

$$\begin{aligned} H_\sigma = \sum_{k\in \mathrm{BZ}} \epsilon_k c^\dagger_{k\mathrm{B}\sigma} c_{k\mathrm{A}\sigma} + \mathrm{h.c.} \\ + \Delta_\sigma \sum_{k\in \mathrm{BZ}} \left(c^\dagger_{k\mathrm{A}\sigma} c_{k\mathrm{A}\sigma} - c^\dagger_{k\mathrm{B}\sigma} c_{k\mathrm{B}\sigma} \right) \end{aligned} \tag{10}$$

where we have employed a Fourier transform in the two sublattices and correspondingly we have defined the complex function:

$$\epsilon_k = \sum_\mu \mathrm{e}^{\mathrm{i}\boldsymbol{\xi}_\mu \cdot \boldsymbol{k}}. \tag{11}$$

In the square lattice case the presence of the next-nearest hopping implies a further term:

$$H_{t'} = \sum_{k\in \mathrm{BZ},\sigma} \epsilon'_k (c^\dagger_{k\mathrm{A}\sigma} c_{k\mathrm{A}\sigma} + c^\dagger_{k\mathrm{B}\sigma} c_{k\mathrm{B}\sigma}) \tag{12}$$

with $\epsilon'_k = 4t' \cos k_x \cos k_y$ to be added to H_σ in equation (10). For a uniform solution in both sublattices the average spin densities are given by:

$$\langle SD_\downarrow|n_{\downarrow,R}|SD_\downarrow\rangle = \begin{cases} \rho_{\mathrm{A}\downarrow} & \text{for } R \in \mathrm{A} \\ \rho_{\mathrm{B}\downarrow} & \text{for } R \in \mathrm{B} \end{cases} \tag{13}$$

$$\langle SD_\uparrow|n_{\uparrow,R}|SD_\uparrow\rangle = \begin{cases} \rho_{\mathrm{A}\uparrow} & \text{for } R \in \mathrm{A} \\ \rho_{\mathrm{B}\uparrow} & \text{for } R \in \mathrm{B}. \end{cases} \tag{14}$$

The parameters $\Delta_\uparrow$ and $\Delta_\downarrow$, defining the Hartree-Fock Hamiltonians are given therefore by:

$$\Delta_\uparrow = \frac{\Delta}{2} + \frac{U}{2}(\rho_{\mathrm{A}\uparrow} - \rho_{\mathrm{B}\uparrow}) \tag{15}$$

$$\Delta_\downarrow = \frac{\Delta}{2} + \frac{U}{2}(\rho_{\mathrm{A}\downarrow} - \rho_{\mathrm{B}\downarrow}). \tag{16}$$

The constant is obtained after little algebra

$$\begin{aligned} E_{\mathrm{const}} = \frac{U}{2}(\rho_{\mathrm{A}\uparrow} + \rho_{\mathrm{B}\uparrow})N_\downarrow + \frac{U}{2}(\rho_{\mathrm{A}\downarrow} + \rho_{\mathrm{B}\downarrow})N_\uparrow \\ - \frac{UL}{2}(\rho_{\mathrm{A}\uparrow}\rho_{\mathrm{A}\downarrow} + \rho_{\mathrm{B}\uparrow}\rho_{\mathrm{B}\downarrow}) \end{aligned}$$

where $N_\uparrow$ and $N_\downarrow$ are the total number of spin up and spin down particles ($N_\uparrow = N_\downarrow = L/2$). At one electron per site all the bonding bands $E_{k,\sigma} = -\sqrt{|\epsilon_k|^2 + \Delta_\sigma^2}$ are occupied by the spin up and spin down electrons and the total Hartree-Fock energy is

$$E_{\mathrm{tot}} = E_{\mathrm{const}} + \sum_{k\in \mathrm{BZ}\sigma} E_{k,\sigma}. \tag{17}$$

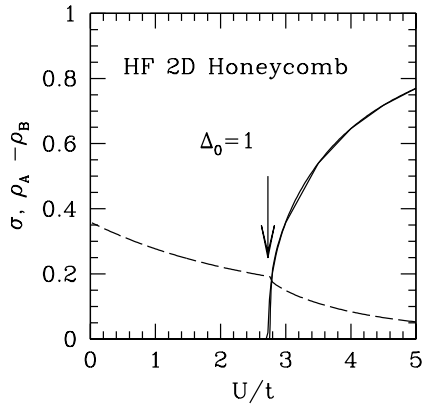

Fig. 5. Honeycomb lattice, Hartree-Fock calculation of the staggered magnetization σ and the density difference $\rho_A - \rho_B$. The transition is 2nd order. The arrow indicates the transition point.

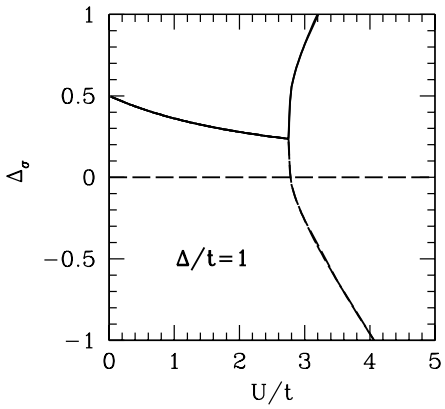

Fig. 6. Honeycomb lattice, Hartree-Fock calculation of the effective energy gap Δ_σ. Two different critical values U_{c1}, U_{c2} of the interaction are identified. Below U_{c1} there is only a solution with $\Delta_\uparrow = \Delta_\downarrow$. Above U_{c1} a solution with $\Delta_\uparrow \neq \Delta_\downarrow$ exists leading to a finite value of the magnetization σ. One of the spin bands becomes gapless at a slightly different value of the interaction U_{c2}.

By minimizing the total energy we obtain two self consistent equations for the variational parameters Δ_σ:

$$\Delta_\sigma = \frac{\Delta}{2} - \frac{\Delta_{-\sigma}}{L} \sum_{k \in \mathrm{BZ}} \frac{1}{E_{k,-\sigma}} \cdot \tag{18}$$

These equations can be easily solved by inserting a trial initial value for $\Delta_\uparrow$ and $\Delta_\downarrow$ in the rhs and iterating the result until selfconsistency is reached. For small U only a self consistent solution with $\Delta_\uparrow = \Delta_\downarrow$ is possible, with a small charge transfer from the electron-rich site B to the electron-poor site A. The plot of the quantity $\rho_A - \rho_B = (\Delta_\uparrow + \Delta_\downarrow - \Delta)^2/U$, is shown in Figure 5.

For large U a broken symmetry solution with $\Delta_\uparrow \neq \Delta_\downarrow$ is possible for U sufficiently large. A finite value of the staggered magnetization $\sigma = \frac{1}{2}(\rho_{A\uparrow} - \rho_{A\downarrow} - \rho_{B\uparrow} + \rho_{B\downarrow})$ is stable, and is given by:

$$\Delta_\downarrow - \Delta_\uparrow = U\sigma.$$

For large enough U, Δ can be neglected and we approach asymptotically the standard antiferromagnetic solution, where

$$\Delta_\uparrow = -\Delta_\downarrow.$$

It is clear therefore that after the magnetic transition, which occurs first in HF, there is a slightly larger critical U when one of the two bands becomes gapless with $\Delta_\sigma = 0$. A plot of the Hartree-Fock band gaps $\Delta_\uparrow$ and $\Delta_\downarrow$ is shown in Figure 6. The self consistent equations (18) for the 2D square lattice case are not modified by the presence of t' at least in the insulating HF phases where the bonding bands $E^B_{k,\sigma} = \epsilon'_k - E_{k,\sigma}$ are full and the antibonding bands $E^A_{k,\sigma} = \epsilon'_k + E_{k,\sigma}$ are empty for both spin up and down electrons. However for $t' \neq 0$ we found a finite U interval – between the band insulator at small U and the Mott-Hubbard insulator at large U – where the bonding and the antibonding bands do overlap in a finite energy range, leading to a fully metallic behavior (see Fig. 7). Here the above analysis should be slightly modified to take into account the gain in energy obtained by occupying some states of the antibonding band.

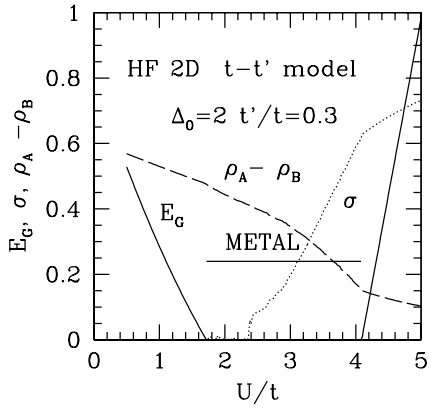

Fig. 7. Square lattice with nearest neighbour hopping: HF calculation of the staggered magnetization σ, the density difference $\rho_A - \rho_B$ and the band insulator gap E_G

Although the Hartree-Fock approximation is by no means exact, it certainly represents a good starting point in dimension larger than one, so that we expect the tt' model to have indeed an extended metal phase between the two insulators. We will not study the square lattice tt' model further, since the general three-phase sequence: band insulator – extended metal phase – Mott-Hubbard insulator is not our main concern.

According to Hartree-Fock, the two insulator phases are however still adjacent on the two sides of U_c in the square lattice with first neighbour hopping ($t' = 0$), and in the honeycomb lattice, with any hopping. In the former, the nesting property of the non interacting Fermi surface affects dramatically the HF solution, making it effectively one-dimensional, and leading to an unphysical first order transition [4]. Moreover, even beyond Hartree-Fock, the first-neighbour square lattice model is not generic enough.

An arbitrarily small next neighbour hopping will take it away to a tt', where the two insulators are most likely no longer adjacent.

We conclude that, at least at the HF level, the simplest model which generically possesses a transition between a Mott and a band insulator in 2D is the honeycomb lattice. Here i) the HF transition to a magnetic phase is second order; ii) there is no nesting of the non interacting Fermi surface, which consists of just two k-points; and iii) the HF solution is always insulating (band or Mott) as a function of U with the exception of a point where there is semimetallic behavior. For the above reasons, rather well justified at the HF level, in 2D we shall restrict our study to the honeycomb lattice case.

In the honeycomb HF solution, there is a small difference between the two critical values of U, one where magnetism sets in, and the next where a band gap closes (Fig. 6). Bearing in mind the discussion of Section 3.2, we cannot judge whether this difference and its sign is just an artifact of the HF calculation or a real one. Because of the crudeness of Hartree-Fock, most likely the second.

The evolution of the full Hartree-Fock band structure for increasing U (not shown) is also instructive. The bands display a full gap both in the band insulator, and in the magnetic insulator. The presence of a spin gap in the latter is clearly an artifact due to breaking of spin rotation invariance characteristic of Hartree-Fock. At the upper critical U, where the charge gap closes, there is linear band dispersion, a point-like Fermi surface, and a Dirac massless spectrum centered at the 2D zone boundary. Therefore we could expect a semimetallic state to exist at the threshold between the two different insulators.

4.1 Nature of the 2D polarization anomaly in the 1D and 2D honeycomb lattice

We argue that close to the point where the effective gap $\Delta_\downarrow$ changes sign, the polarization will change dramatically as a function of U. To verify our statement, we make use of the theory of the polarization, in the geometric phase formulation [5–7,17]. In the Hartree-Fock case, this amounts to calculate the contribution to the polarization of the spin-polarized band which becomes gapless at the critical point, when one effective gap parameter changes sign. In order to better illustrate that, we consider a model system consisting of spinless noninteracting fermions, described by the Hamiltonian (10) with a density of 1/2 fermion per site. With periodic boundary conditions, we can calculate analytically the change of polarization as we vary continuously the fermion energy gap Δ, or alternatively as we introduce a small dimerizing distortion δ in the hopping. In the linear chain, without any distortion, $\delta \to 0$, the variation of the polarization as a function of the energy difference Δ between anions and cations is described by a step function: $P_0(\Delta) = \frac{ea}{4}\frac{\Delta}{|\Delta|}$ (see Ref. [7]). When we vary Δ without changing its sign, the polarization does not change, while when the sign changes, the polarization jumps by $\frac{ea}{2}$ as anticipated. We introduce a dimerizing distortion ("optical phonon-like") δ which amounts to a change of the hopping $t \to t(1 \pm \delta)$ for electrons hopping to the right and the left respectively of any B site. We can evaluate analytically the "Born effective charge", which is the derivative of the polarization with respect to δ at $\delta = 0$:

$$\lim_{\delta \to 0} P'_\delta(\Delta) = \frac{ea}{2\pi}\{k'K - \frac{1}{k'}(2K + E)\} \tag{19}$$

where $k = (1+\frac{\Delta^2}{16t^2})^{-1/2}$, $k' = \frac{\Delta}{4t}(1+\frac{\Delta^2}{16t^2})^{-1/2}$. $K = K(k)$ and $E = E(k)$ are complete elliptic functions of the first and second kind.

In this model, we have thus recovered the divergent effective charge anomaly discovered numerically in the 1D many-body calculation of Resta and Sorella [3]. The same analysis holds for two-dimensional or higher d-dimensional lattices provided that at the transition point $\Delta = 0$ the bonding and the antibonding bands touch at a $d-1$-dimensional (Fermi-) surface, (nesting). That is the case in particular for the $D = 2$ square lattice but not for the honeycomb lattice.

In the honeycomb lattice, using the geometric phase technique for the mentioned spinless fermion model, it is straightforward to verify that without any distortion the polarization does not change as we vary Δ. Introducing a distortion along the ξ_1 direction: $t_0 = t_2 = t(1-\delta)$, $t_1 = t(1+2\delta)$, one can then verify that the component of the change in polarization which is orthogonal to ξ_1 vanishes, at least in first order in δ.

Along ξ_1, it is difficult to derive an analytic expression for the change in polarization. We can however extract the singular part of the effective charge, in the neighbourhood of the zero of Δ

$$\lim_{\substack{\delta \to 0 \\ \Delta \to 0}} P'_\delta(\Delta) = \frac{ea}{2\pi}\frac{\Delta}{|\Delta|}\,. \tag{20}$$

The effective charge has therefore a finite symmetric jump when Δ changes sign. Since this is only the singular part, there will be in addition a smooth background contribution shifting this jump with respect to zero. (In $D = 1$, the singularity was infinite, so there the shift was irrelevant.)

In conclusion, if the Hartree-Fock approximate picture were correct, we should expect such a polarization jump to emerge in the full many-body calculation for the 2D honeycomb lattice of the next section. As it will turn out, the jump is indeed verified (see Fig. 8). Moreover, the quantitative size of the jump is remarkably close to twice the value we have just obtained analytically. This result may be understood by assuming that each of the two bands with opposite spins, are forced to close together their single particle gaps, due to the spin rotation invariance of the model. This also suggests that the jump in the effective charge in 2D, similarly to the jump in the polarization in 1D, maybe due to topological reasons and therefore rather general and weakly dependent on the parameters defining the model.

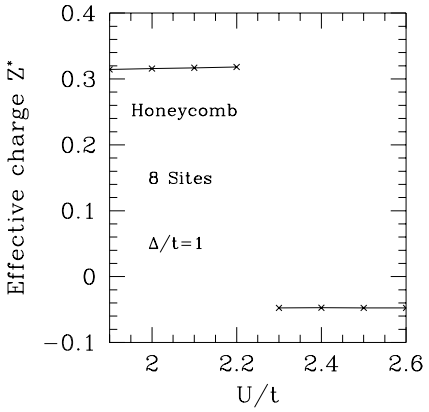

Fig. 8. Honeycomb lattice, plot of the effective charge Z^* as a function the Hubbard onsite interaction U for $\Delta = 1$. The effective charge shows a finite jump at U_c unlike the 1D case where the jump diverged.

5 2D honeycomb lattice: many-body calculation of the polarization

We now proceed to do proper polarization – or more precisely, effective charge – calculation for a 2D interacting case. We restrict our study of the Hamiltonian (1) to the honeycomb lattice (a sort of 2D hexagonal BN), which is slightly more interesting because it does not possess inversion symmetry, and can have, *e.g.*, a piezoelectric effect (see Sect. 6). The sites of the A sublattice are given by $R_A = R_{m,n}$, with $R_{m,n} = (\frac{3}{2}n + 3m, \frac{\sqrt{3}}{2}n)a$, a is the lattice constant and $1 \le n \le N_y$, $1 \le m \le \frac{N_x+2}{2}$. The lattice is space periodic under translations $T_1 = (\frac{3}{2}, \frac{\sqrt{3}}{2})N_y a$ and $T_2 = (3, 0)\frac{N_x+2}{2}a$. The reciprocal lattice vectors are $G_1 = \frac{4\pi}{\sqrt{3}a}(0, 1)$ and $G_2 = \frac{2\pi}{3a}(1, -\sqrt{3})$. The sites of the B sublattice are given by: $R_B = R_{mn} + \xi_\mu$, $\mu = 0, 1, 2$ where the three vectors ξ_μ which connect neighbouring A and B sites are $\xi_0 = (-\frac{1}{2}, \frac{\sqrt{3}}{2})a$, $\xi_1 = (1, 0)a$ and $\xi_2 = (-\frac{1}{2}, -\frac{\sqrt{3}}{2})a$. Obviously $\xi_0 + \xi_1 + \xi_2 = 0$. We can also consider, for the purpose of mimicking a uniaxial stress along the ξ_1 direction: $t_0 = t_2 = t(1-\delta)$ and $t_1 = t(1+2\delta)$. The Hamiltonian depends parametrically on δ, $H = H(\delta)$. In order to calculate the difference in the polarization of the system as the parameter is varied between its values 0 and δ, we consider families of Hamiltonians $H_k(\delta)$ obtained from (1) by introducing a complex hopping and substituting $t_\mu \to t_\mu e^{ik\cdot\xi_\mu}$, where the parameter k is given by $k = k_1 G_1 + k_2 G_2$, with $0 \le k_\alpha < 1$, $\alpha = 1, 2$. This is equivalent to imposing generalised boundary conditions on the original Hamiltonian [18]: If $\psi(r_1, \dots, r_j, \dots)$ is an eigenfunction of H, then generalized boundary conditions imply $\psi(r_1, \dots, r_j + T_\alpha, \dots) = e^{i2\pi k_\alpha}\psi(r_1, \dots, r_j, \dots)$, $\alpha = 1, 2$. Periodic boundary conditions correspond to $k_\alpha = 0$, antiperiodic to $k_\alpha = 1/2$. The polarization difference between two states which are characterised by the initial and final value of the distortion, 0 and δ is given as an integral over the generalised boundary conditions:

$$\Omega\, G_\alpha\, \Delta P = e \int_0^1 \mathrm{d}k_\beta \big(\Gamma_\alpha(\delta) - \Gamma_\alpha(0)\big) \tag{21}$$

where Ω is the unit cell volume, α and β take alternatively the values 1 or 2, $\Gamma_\alpha(\delta)$ is the many-body generalisation of the geometric phase:

$$\Gamma_\alpha(\delta) = \mathrm{i} \int_0^1 \mathrm{d}k_\alpha \langle \Phi_0(\delta, k)| \frac{\partial}{\partial k_\alpha} \Phi_0(\delta, k)\rangle \tag{22}$$

and $\Phi_0(\delta, k)$ is the ground state of $H_k(\delta)$, which satisfies periodic boundary conditions.

In the numerical calculation, we adopt a cell with 8 lattice sites ($N_x = N_y = 2$) and 8 electrons. The number of spin-up and spin-down electrons is 4, and the dimension of the Hilbert space is only 4 900. The system is really very small, but we expect that averaging over the boundary conditions will reduce the finite size effects. In the calculation we are interested to study the behaviour of ΔP, the polarization difference between the undistorted ($\delta = 0$) and the distorted ($\delta \neq 0$) case, for different values of the onsite interaction U.

We use a discretized form to calculate the geometric phase numerically

$$\Gamma_\alpha(\delta) = -\mathrm{i} \ln \prod_{j=0}^{N_\alpha - 1} \frac{\langle \Phi_0(\delta, (\frac{j}{N_\alpha}, k_\beta))|\Phi_0(\delta, (\frac{j+1}{N_\alpha}, k_\beta))\rangle}{|\langle \Phi_0(\delta, (\frac{j}{N_\alpha}, k_\beta))|\Phi_0(\delta, (\frac{j+1}{N_\alpha}, k_\beta))\rangle|}\,. \tag{23}$$

The geometric phase however is only defined modulo 2π and an uncertainty in the result for the difference in polarization arises. There will be an ambiguity in the value of the polarization difference up to a quantum. However the polarization difference should remain unambiguous for neighbouring values of δ. We can thus fix the 2π uncertainty in $\Gamma(\delta)$ by requiring that $\Gamma(\delta)$ is continuous in δ for a given value of U. We may also require that it is continuous for neighbouring values of U for fixed δ, so long as we do not cross a point of degeneracy in the electronic spectrum.

Convergence in the integration with respect to k_β has not been easy and we had to use grids with 150 or 300 points to get reliable results. At the end we found that in the undistorted case, similarly to the one-dimensional case, there is a critical point U_c, where the geometric phase changes discontinuously by π for one k_β in the 2D Brillouin zone. As in one dimension this effect maybe related to the presence of a level crossing as a function of U/t for a particular boundary condition. Introducing next the dimerizing distortion, we found that the effective charge, as in the one-dimensional case, is positive in the region below U_c and negative above. At U_c it is discontinuous, with a finite jump, instead of the one-dimensional divergence. A plot of the effective charge as a function of U/t is shown in Figure 8.

6 Piezoelectric inversion, and concluding remarks

The transition between an ionic band insulator and a Mott-Hubbard insulator as exhibited by the prototype model (Eq. (1)) is quite interesting. We have extended existing studies in $D = 1$, probing deeper into the transition. We have also carried out newer investigations in $D = 2$, where same kind of transition is shown to take place, with some differences between the square and the honeycomb lattice.

With reference to the list of questions presented in the introduction, we can now formulate the following answers.

1. The physical origin of the polarization anomaly is connected with the symmetry switch between an even state, typical of the band insulator, to an odd state, typical of the Mott insulator. The symmetry switch, which we [3] and others [4] had noted earlier for finite size, is established here for arbitrary size. Moreover, in $D = 1$, even and odd refer to simple inversion symmetry, in $D = 2$ the pertinent symmetry operation is different and depends on the lattice.

2. The threshold state between the ionic and the Mott insulator, where the polarization abruptly changes sign, is one where the charge gap seems to close, and is therefore metallic. This result underlines the profound difference between the two types of insulator, and invites further studies, which are now beginning to appear [14] of this transition.

3. In $D = 2$ the same model has again a band-to-Mott insulator transition. The polarization anomaly is generally weaker, to a degree which depends on the lattice. In one dimension the effective charge diverges at the transition undergoing an abrupt sign change from $+\infty$ to $-\infty$. In two dimensions this sign change persists. We have shown that in the 2D honeycomb lattice the divergence turns to a jump, again with a change of sign. Here the magnitude of this jump is found to coincide almost exactly with ea/π, suggesting that this jump could be an experimentally detectable quantity dependent only on the bulk lattice constant and no other details of the actual material.

4. The total piezoelectric coefficient γ might be used to detect the polarization anomaly, because it is sensitive to the sign of Z^*. It is conventionally divided into two contributions: the first, γ_0, is purely electronic, and is related to a uniform stress of the solid (a simple scaling of all distances in the unit cell); the second, more important contribution, is obtained by keeping the unit cell fixed and by changing the distance between atoms. In lattices without inversion symmetry, the piezoelectric coefficient γ is directly proportional, in magnitude and sign, to the effective charge Z^*, in the form (we omit here for simplicity tensorial and vectorial indices) [19,20]

$$\bar{\gamma} = \gamma_0 + Z^* \xi \tag{24}$$

where the constant ξ represents the internal strain parameter.

An anomaly in Z^* will clearly reflect in the piezoelectric coefficient. Piezoelectric measurements could therefore permit the detection of a band-to-Mott insulator transition, provided the system does not possess inversion. The honeycomb lattice which we have studied in $D = 2$ is the simplest one that does not possess inversion symmetry. Our study shows that the transition is not suppressed by piezoelectric strain.

We have not been able to identify, at present, a likely compound where this kind of transition could be experimentally detected. It would seem possible, nevertheless, that suitable systems could be engineered, especially in the organic world.

We are thankful to M. Fabrizio, S. de Gironcoli, A. Parola, R. Resta and K. Schönhammer for useful discussions. N.G. acknowledges financial support through an EEC fellowship under the HCM Programme Contract No. ERBCHBGCT940721. Work at SISSA was co-sponsored by INFM through PRA HTSC, and by the European Union through Contract ERBCHRXCT940438. Part of the calculations were performed during N.G.'s visit to CINECA, under the Icarus2 project, Contract No. ERBFMGECT950052. S. Cozzini is acknowledged for his help with the parallelization of the codes.

References

1. N. Nagaosa, J. Takimoto, J. Phys. Soc. Jpn **55**, 2735 (1986); 2745.
2. T. Egami, S. Ishihara, M. Tachiki, Science **261**, 1307 (1993).
3. R. Resta, S. Sorella, Phys. Rev. Lett. **74**, 4738 (1995).
4. G. Ortiz, P. Ordejón, R.M. Martin, G. Chiappe, Phys. Rev. B **54**, 13515 (1996).
5. R.D. King-Smith, D. Vanderbilt, Phys. Rev. B **47**,1651 (1993).
6. R. Resta, Ferroelectrics **136**, 51 (1992); Rev. Mod. Phys. **66**, 889 (1994).
7. G. Ortiz, R.M. Martin, Phys. Rev. B **49**, 14202 (1994).
8. G. Baskaran, Z. Zou, P.W. Anderson, Solid State Commun. **63**, 973 (1987).
9. See *e.g.* L. Faddeev, L. Takhtajan, Phys. Lett. A **85**, 375 (1981) and references therein.
10. J.D. Reger, A.P. Young, Phys. Rev. B **37**, 5978 (1988).
11. K.J. Runge, Phys. Rev. B **45**, 7229; 12292 (1992).
12. S. Chakravarty, B. Halperin, D. Nelson, Phys. Rev. Lett. **60**, 1057 (1988); Phys. Rev. B **39**, 2344 (1989).
13. E. Lieb, D. Mattis, J. Math. Phys. **3**, 749 (1962).
14. M. Fabrizio, A.O. Gogolin, A.A. Nersesyan, Phys. Rev. Lett. **83**, 2014 (1999).
15. A finite size gap minimum, which we believe is compatible with charge gap closing in the thermodynamic limit, was obtained in a 64-site DMRG calculation by K. Schönhammer, O. Gunnarson, R.M. Noack, Phys. Rev. B **52**, 2504 (1995). We are grateful to Professor Schönhammer for pointing out this reference to us.
16. A. Parola (private communication).
17. D. Vanderbilt, R.D. King-Smith, Phys. Rev. B **48**, 4442 (1993).
18. C. Gros, Phys. Rev. B **53**, 6865 (1996), Z. Phys. B **86**, 359 (1992).
19. R.M. Martin, Phys. Rev. B **5**, 1607 (1972).
20. S. de Gironcoli, S. Baroni, R. Resta, Phys. Rev. Lett. **62**, 2853 (1989).